
Robust Heterogeneous Analog-Digital Computing for Mixture-of-Experts Models with Theoretical Generalization Guarantees

Mohammed Nowaz Rabbani Chowdhury¹ Hsinyu Tsai² Geoffrey W. Burr² Kaoutar El Maghraoui² Liu Liu¹
Meng Wang¹

Abstract

Sparse Mixture-of-Experts (MoE) models enable efficient scalability by activating only a small subset of experts per input, yet their massive parameter counts lead to substantial memory and energy inefficiency during inference. Analog in-memory computing (AIMC) offers a promising solution by eliminating frequent data movement between memory and compute units. However, mitigating hardware nonidealities of AIMC typically requires noise-aware retraining, which is infeasible for large MoE models. In this paper, we propose a retraining-free heterogeneous computation framework in which noise-sensitive experts, which are provably identifiable by their *maximum neuron norm*, are computed digitally while the majority of the experts are executed on AIMC hardware. We further assign densely activated modules, such as attention layers, to digital computation due to their high noise sensitivity despite comprising a small fraction of parameters. Extensive experiments on large MoE language models, including DeepSeekMoE and OLMoE, across multiple benchmark tasks validate the robustness of our approach in maintaining accuracy under analog nonidealities.

1. Introduction

The sparse computation of Mixture-of-Experts (MoE) models allows efficient scaling of large language and vision models without the proportional increase of training compute (Shazeer et al., 2017; Riquelme et al., 2021; Fedus et al., 2022; Chowdhury et al., 2023). For each input token, the model activates only a small subset of group of neurons in the feed forward network (FFN) modules of Transformer. Each of the group is referred to as an *expert*. Due to their

excellent scalability, modern MoE-based large language models (LLMs) have grown to disproportionately large parameter sizes (Jiang et al., 2024; Guo et al., 2025; Yang et al., 2025), which in turn require substantial memory to operate and result in significant energy inefficiency while computing in digital accelerators (Frantar & Alistarh, 2024; Chowdhury et al., 2024; Jegham et al., 2025; Fernandez et al., 2025).

The analog in-memory computing (AIMC) provides a promising solution to the inefficiencies of MoE (Büchel et al., 2025b). AIMC allows to compute the matrix-vector multiplication (MVM) inside the non-volatile memory (NVM) devices, thus eliminating the need for frequent movement of large expert parameters between the memory and compute units, which is the major source of energy inefficiency (Burr et al., 2017; Joshi et al., 2020; Sebastian et al., 2020; Fujiwara et al., 2024). However, MVM operations on AIMC hardware are inherently approximate due to various nonidealities, such as noise introduced by digital-to-analog and analog-to-digital conversions (DAC and ADC) and inaccuracies in programming weights onto NVM devices (Hou et al., 2025). These nonidealities can lead to substantial degradation in model performance. A common strategy to alleviate this degradation is noise-aware retraining, which improves robustness to AIMC-induced noise (Rasch et al., 2023; Büchel et al., 2025a). However, the large parameter counts of modern MoE models renders such retraining approaches impractical for AIMC deployment.

For a robust retraining-free deployment of large MoE models in AIMC requires a heterogeneous computing approach, where the most sensitive components (e.g., noise-sensitive experts) are computed in digital accelerators, and the rest of the model components are computed in AIMC devices. However, a systematic approach is required to identify the noise-sensitive model components for the pareto-optimal heterogeneous deployment. This raises a fundamental questions:

How to identify the noise-sensitive model components for the heterogeneous Digital-AIMC deployment of MoE?

In this paper, we address the question both theoretically

¹Rensselaer Polytechnic Institute ²IBM Research. Correspondence to: Mohammed Nowaz Rabbani Chowdhury <chowdm2@rpi.edu>, Meng Wang <wangm7@rpi.edu>.

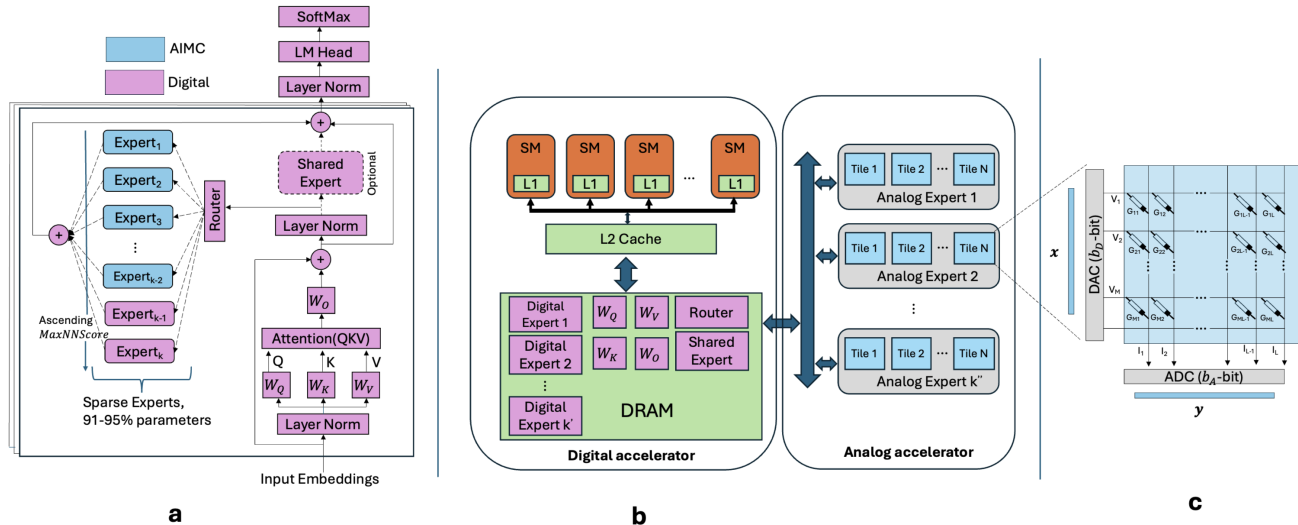


Figure 1. **a.** In heterogeneous computing of MoE, the dense modules and noise-sensitive expert modules are computed in a digital accelerator while rest of the experts are computed in an analog accelerator. **b.** A schematic of digital and analog accelerator. **c.** The analog accelerator is comprised of non-volatile memory (NVM) tiles. Weights are programmed to the crossbar array of the tile.

and empirically. Our theoretical analysis reveals that the experts composed of neurons with large ℓ_2 -norms are more susceptible to weight-programming noise in AIMC. We therefore propose to compute these experts in digital, while computing rest of the experts in AIMC devices. We further propose to compute the dense model components (e.g., the multi-head self-attention modules, the language modeling head, and the shared experts (if any) of MoE-LLMs) in digital due to their high per-parameter sensitivity to analog noises. We summarize our main contributions as follows:

1. The first analog noise-sensitivity analysis of large MoE models. To the best of our knowledge, this paper provides the first systematic sensitivity analysis of different model components in large MoE models under the two major sources of AIMC nonidealities: the DAC-ADC noise, and the weight-programming noise. Our analysis reveals that a subset of experts exhibits pronounced performance degradation as weight-programming noise increases, suggesting the computation of these experts in digital. Furthermore, we show that dense model components in MoE—despite accounting for only a small portion of the total parameters—are highly sensitive to both DAC-ADC and weight-programming noise due to their involvement in processing all input tokens.

2. A theoretically grounded metric—the expert maximum neuron norm score—for digital expert selection. We theoretically prove that, the experts specializing in frequently appearing important tokens in data contain neurons with large ℓ_2 norms, hence demonstrate high sensitivity to weight-programming noise. We therefore propose to compute the experts with large maximum neuron norm scores—defined as the product of the maximum neuron

ℓ_2 norms across all linear projection layers within an expert—in digital.

3. Empirical validation of the proposed heterogeneous computing approach on large MoE models. We empirically evaluate the proposed heterogeneous computing framework on large-scale MoE models, including DeepSeekMoE (Dai et al., 2024) (16B parameters) and OLMoE (Muenighoff et al., 2025) (7B parameters), across a diverse set of benchmark LLM tasks. The results demonstrate that our maximum neuron norm-based digital expert selection consistently outperforms prior expert selection strategies proposed in the MoE literature, demonstrating robustness in maintaining accuracy under imperfect analog computation.

1.1. Related Works

Analog in-memory computing of large models. The evaluation of in-memory computing performance is largely limited to smaller size models of different architectures such as CNNs (Joshi et al., 2020; Gokmen et al., 2019), RNNs (Rasch et al., 2023), LSTMs (Tsai et al., 2019), and encoder only Transformers (Spoon et al., 2021). (Zhang et al., 2024) minimize DAC-ADC noise for LLMs through activation-shifting and weight-resaping. (Büchel et al., 2025a) conduct large scale noise-aware retraining for foundation LLMs. (Hou et al., 2025) conduct sensitivity analysis of LLMs on various analog noise sources and proposes a training-free rescaling method to mitigate the noise. In all of the cases, the model sizes (1-3B) are well below typical MoE parameter ranges.

Efficient inference of Mixture-of-Experts. Due to the large memory requirements of MoE, inference cost reduc-

tion has drawn much attention recently (Koishekenov et al., 2023; Li et al., 2024b; Chowdhury et al., 2024; Frantar & Alistarh, 2024; Huang et al., 2025). Most of the works focus on expert pruning and quantization to mitigate inference cost. (Büchel et al., 2025b) demonstrate improved scalability of MoE in 3D AIMC architecture compared to dense models.

Theoretical generalization guarantees of neural networks. Due to high non-convexity, the theoretical generalization analysis of neural networks is mostly limited to two-layers (Chowdhury et al., 2023; Bu et al., 2024; Li et al., 2025b). Feature learning dynamics is widely used to gain insights about different training and inference properties (Li et al., 2024a; 2025a). Most works require simplified data model to facilitate analysis (Brutzkus et al., 2018; Karp et al., 2021; Shi et al., 2022).

2. Background

2.1. The Mixture-of-Experts Architecture

An MoE block replaces the dense feed-forward network (FFN) of a Transformer layer with a set of sparsely activated FFN modules, referred to as *experts*. A routing network determines which experts are activated for each input token, enabling conditional computation. Common routing strategies include *token-choice routing* (Fedus et al., 2022), where each token selects its top experts, and *expert-choice routing* (Zhou et al., 2022), where each expert selects a subset of tokens.

For an MoE block with k experts, each expert $s \in [k]$ is implemented as a two-layer MLP or gated MLP with projection matrices $\mathbf{W}_{\text{up}}^{(s)} \in \mathbb{R}^{d \times m}$ and $\mathbf{W}_{\text{down}}^{(s)} \in \mathbb{R}^{m \times d}$. In the gated-MLP variant, an additional gate-projection matrix $\mathbf{W}_{\text{gate}}^{(s)} \in \mathbb{R}^{d \times m}$ is used. The routing network is parameterized by a routing matrix $\Sigma \in \mathbb{R}^{d \times k}$.

Given an input token $\mathbf{x} \in \mathbb{R}^d$, the routing network computes routing scores $\mathbf{x}^\top \Sigma$. A sparse subset of experts is activated according to the chosen routing strategy and the input \mathbf{x} , and the output token is computed as $\mathbf{x}_{\text{out}} = \sum_{s \in \mathcal{A}} \mathbf{f}_s(\mathbf{x})$, where $\mathcal{A} \subseteq [k]$ denotes the set of activated experts and $\mathbf{f}_s(\cdot)$ is the expert function.

For a standard MLP expert,

$$\mathbf{f}_s(\mathbf{x}) = G^{(s)} [\phi(\mathbf{x}^\top \mathbf{W}_{\text{up}}^{(s)}) \mathbf{W}_{\text{down}}^{(s)}]^\top, \quad (1)$$

and for a gated-MLP expert,

$$\mathbf{f}_s(\mathbf{x}) = G^{(s)} [(\phi(\mathbf{x}^\top \mathbf{W}_{\text{up}}^{(s)}) \odot (\mathbf{x}^\top \mathbf{W}_{\text{gate}}^{(s)})) \mathbf{W}_{\text{down}}^{(s)}]^\top. \quad (2)$$

Here, $\phi(\cdot)$ denotes an element-wise activation function, \odot denotes the Hadamard product, and $G^{(s)}$ is the routing

weight for expert s , obtained by normalizing routing scores as specified by the routing mechanism.

2.2. Analog In-Memory Computing of Neural Networks

In the analog in-memory computing (AIMC) paradigm, the matrix-vector multiplication (MVM) of a linear layer is performed in non-volatile memory (NVM) devices (e.g., PCM (Joshi et al., 2020), ReRAM (Wan et al., 2022)), where weights are programmed as NVM cell conductances. Digital inputs are converted to analog signals via a digital-to-analog converter (DAC), and the resulting column currents, representing the analog output, are converted back to digital by an analog-to-digital converter (ADC) for subsequent digital operation.

The MVM operation in AIMC accelerators is not exact. The nonidealities arises from the weight programming noise and other system-level nonidealities, as well as the quantization noise in DAC and ADC. The programming noise and the DAC-ADC noise dominate over other system-level noises.

The weight programming noise. The weight programming noise arises from the imprecise programming of weights in NVM devices. (Le Gallo et al., 2023) proposes a mathematical model to characterize this noise, as shown in (3),

$$\hat{W}_{i,j} = W_{i,j} + \mathcal{N}(0, \sigma_{i,j}^2), \sigma_{i,j} = c_0 W_{\text{max}} + \sum_{u=1}^3 c_u \frac{|W_{i,j}|^u}{W_{\text{max}}^{u-1}} \quad (3)$$

Here, $W_{i,j}$ is the j -th element of the column i in the NVM tile, W_{max} is the maximum weight-magnitude of the column. This model shows that the noisy weight $\hat{W}_{i,j}$ is the sum of the original weight $W_{i,j}$ and a zero-mean Gaussian noise that depend on $W_{i,j}$ and W_{max} . For example, (Le Gallo et al., 2023) fits (3) using the data obtained from a state-of-the-art 64-core PCM-based AIMC chip, and obtain $c_0 = 0.012, c_1 = 0.245, c_2 = -0.54, c_3 = 0.40$ if $W_{i,j} > 0.292 \times W_{\text{max}}$, and $c_0 = 0.014, c_1 = 0.224, c_2 = -0.72, c_3 = 0.952$ otherwise.

DAC-ADC noise. DAC noise originates from quantizing floating-point digital inputs (typically FP16) to b_D -bit integers representing discrete analog levels. For a fixed input range β_{in} , the quantized input is

$$x_q := \frac{\beta_{\text{in}}}{2^{b_D-1} - 1} \left[\text{clamp}(x, -\beta_{\text{in}}, \beta_{\text{in}}) \frac{2^{b_D-1} - 1}{\beta_{\text{in}}} \right], \quad (4)$$

where $\text{clamp}(x, a, b) = \min(\max(x, a), b)$. ADC noise arises from quantizing the continuous column currents to b_A -bit digital outputs. For a fixed output range β_{out} , the i -th

column output $y^{(i)}$ of the tile is quantized to

$$y_q^{(i)} := \text{clamp}\left(\frac{\beta_{\text{out}}}{2^{b_A-1}-1} \left\lfloor y^{(i)} \frac{2^{b_A-1}-1}{\beta_{\text{out}}} \right\rfloor, -\beta_{\text{out}}, \beta_{\text{out}}\right),$$

$$\beta_{\text{out}} := \lambda \beta_{\text{in}} \max(|\mathbf{W}_{:,i}|), \quad (5)$$

where $\mathbf{W}_{:,i}$ are the column weights and λ is a tunable hyperparameter.

DAC-ADC calibration. In practice, we can mitigate DAC-ADC noise by calibrating the hyperparameters β_{in} in (4) and λ in (5). For each NVM tile, we set $\beta_{\text{in}} = \kappa \cdot \text{std}(x)$, where $\text{std}(x)$ is the exponential moving average of the input standard deviation over a calibration dataset. The global hyperparameters κ and λ are then calibrated across all tiles over the dataset.

3. The Proposed Heterogeneous Computation of MoE

Before we describe our method of heterogeneous computation of MoE, we first introduce a new metric that we will use to select experts.

Maximum neuron norm score – a metric to select experts. For a projection matrix $\mathbf{W} \in \mathbb{R}^{d \times m}$ with m neurons, we define the maximum neuron norm of this matrix \mathbf{W} as

$$\text{MaxNNorm}(\mathbf{W}) := \max_{i \in [m]} \|\mathbf{W}_{:,i}\|_2, \quad (6)$$

where $\mathbf{W}_{:,i} \in \mathbb{R}^d$ denotes the weight vector of neuron i .

For expert s , we define the *maximum neuron norm score* of a gated-MLP expert s as the product of the maximum neuron norms of three matrices, $\mathbf{W}_{\text{up}}^{(s)}$, $\mathbf{W}_{\text{down}}^{(s)}$, and $\mathbf{W}_{\text{gate}}^{(s)}$,

$$\text{MaxNNScore}^{(s)} := \prod_{* \in \{\text{up}, \text{down}, \text{gate}\}} \text{MaxNNorm}(\mathbf{W}_*^{(s)}). \quad (7)$$

where the gate term in (7) is omitted when defining the maximum neuron norm score for a standard MLP expert s .

Our **heterogeneous computation strategy for MoE** is summarized in Figure 2. The idea is to assign all densely activated modules and the top Γ fraction of experts (ranked by the maximum neuron norm score) to digital computation, with the remaining experts’ linear modules computed on the AIMC accelerator.

Rationale behind computing dense modules in digital. The number of parameters in the densely activated modules (e.g., multi-head self-attention (MHSA), any shared expert, and LM head in MoE-LLM) is insignificant. Typically, 5-6% parameters resides in these modules in total. On the other hand, the processing of all input tokens by these modules indicates high sensitivity to AIMC noise. Computing

Heterogeneous Computation of MoE

Step 1. Place all densely activated modules on the digital accelerator.

Step 2. Rank experts in each MoE block by the maximum neuron norm score in (7) from high to low.

Step 3. Assign the top Γ fraction experts to the digital accelerator. Compute the remaining experts’ linear modules on the AIMC chip.

Figure 2. The heterogeneous computation strategy for MoE models.

these modules in AIMC suggests a large drop in model performance for a minimal gain in efficiency. We therefore propose to compute them in digital.

Rationale for computing programming-noise-sensitive experts in digital. Unlike DAC-ADC noise, which can be mitigated via higher bit precision (b_D , b_A) and calibration of β_{in} and λ , weight programming noise varies across AIMC devices and cannot be controlled after fabrication. Selecting Γ fraction of experts for digital computation based on their programming-noise sensitivity allows flexible trade-offs between efficiency and model performance across devices.

One major contribution of this paper is that we theoretically justify that the maximum neuron norm score is a valid metric for an expert’s sensitivity to weight-programming noise: a larger score indicates higher sensitivity, motivating placement on the digital accelerator. The formal theoretical analysis will be represented in Section 4.

4. Theoretical Support of Experts Selection

4.1. Key Theoretical Insights

To support our metric for expert selection, we analyze the training dynamics of a simpler MoE model to characterize the properties of different experts and their resulting generalization. We consider an analytical framework where an MoE model is trained on a binary sequence classification task. The class label is determined by a task-relevant token in the sequence. There are two class-relevant tokens under each class. One of them appears more frequently than other in the sequences. We denote the frequency of the *less-frequent* task-relevant token by α , i.e., the *more-frequent* task-relevant token appears with frequency $(1 - \alpha)$. Before presenting formal theorems, here we summarize our key theoretical insights.

1. Experts specialized in learning more-frequent tokens have neurons with large magnitude. We theoretically show that the experts which are specialized in more-frequent

tokens hosts neurons with large l_2 norm. Therefore, these experts are more sensitive to weight-programming noise of AIMC devices.

2. Selecting experts with large maximum neuron norm for digital computation improves noise tolerance. Our analysis reveals that selecting experts with large maximum neuron norm, i.e., large value of MaxNNScore for digital computation allows the remaining analog experts to tolerate higher programming noise. Specifically, selecting a fraction of experts with top MaxNNScore that are specialized in more-frequent tokens allows the remaining experts to tolerate $\Omega(\frac{1-\alpha}{\alpha})$ times higher noise magnitude compared with the tolerable noise magnitude when all experts are computed in analog.

4.2. Analytical Setup

We adopted the same theoretical setup as in (Chowdhury et al., 2026). We briefly describe the setup here.

Analytical model and the learning task. We analyze a simplified MoE model of a single MoE block of standard MLP, trained on a binary sequence classification task. Given a sequence of tokens $\mathbf{X} \in \mathbb{R}^{d \times n}$, where each column $j \in [n]$ represents a token $\mathbf{x}^{(j)} \in \mathbb{R}^d$. The sequence label is denoted by $y \in \{+1, -1\}$. The model output is given by,

$$f(\mathbf{X}) := \frac{1}{d} \sum_{j \in [n]} \mathbf{1}^\top \mathbf{x}_{\text{out}}^{(j)} \quad (8)$$

where $\mathbf{x}_{\text{out}}^{(j)}$ is the j -th output token of the MoE block and $\mathbf{1} \in \mathbb{R}^d$ is the all-ones vector. Each expert’s down-projection matrix is fixed throughout the training and given by $\mathbf{W}_{\text{down}}^{(s)} = a^{(s)} \mathbf{1}^{m \times d}$, where $\mathbf{1}^{m \times d}$ is an all-ones matrix and $a^{(s)} \in \{+1, -1\}$. We consider expert-choice routing, where for each expert s , the tokens corresponding to the top l entries of $[\mathbf{X}^\top \boldsymbol{\Sigma}]_{:,s}$ are routed to that expert. The routing weight of token j , routed to expert s , is evaluated as,

$$G_j^{(s)} = \exp([\mathbf{X}^\top \boldsymbol{\Sigma}]_{j,s}) / \sum_{i \in J_s(\mathbf{X})} \exp([\mathbf{X}^\top \boldsymbol{\Sigma}]_{i,s}) \quad (9)$$

where, $J_s(\mathbf{X})$ is the index set of tokens routed to expert s .

Heterogeneous Computation. To characterize the model under heterogeneous computation, we ignore ADC and DAC noise, as these can be largely mitigated through calibration. For weight-programming noise, we simplify the model in (3) by considering only the first term in $\sigma_{i,j}$, resulting in

$$\hat{W}_{i,j} = W_{i,j} + \mathcal{N}(0, c^2 W_{\text{max}}^2). \quad (10)$$

⁰Our analysis can be extended to the full model in (3), at the cost of additional calculation, without changing the main insights. Therefore, we focus on the simplified model in the analysis.

(10) allows us to vary c to control the noise level.

We consider two scenarios: (i) Fully heterogeneous computation, as described in Figure 2, with the resulting model denoted as $f_H(\mathbf{X})$; (ii) All-experts-in-analog computation, where linear modules of all experts are computed on the AIMC chip, denoted as $f_A(\mathbf{X})$.

Sequence sampling model. Let $(\mathbf{X}, y) \sim \mathcal{D}$, where tokens of \mathbf{X} drawn from an orthonormal set $\mathcal{P} \subset \mathbb{R}^d$. Two vectors $\mathbf{o}_1, \mathbf{o}_2 \in \mathcal{P}$ define the task-relevant set $\mathcal{P}_r = \{\pm \mathbf{o}_1, \pm \mathbf{o}_2\}$; all others are task-irrelevant. Each sequence contains exactly one task-relevant token, determining the label: sequences containing $\pm \mathbf{o}_1$ are labeled $+1$, and those containing $\pm \mathbf{o}_2$ are labeled -1 . Remaining tokens are drawn independently from $\mathcal{P} \setminus \{\mathbf{o}_1, \mathbf{o}_2\}$. With probability $\alpha \in (0, 1/4)$, the task-relevant token is \mathbf{o}_1 or \mathbf{o}_2 .

Training Setup. We analyze the case, where the network given in (8) is trained for T steps via SGD with batch size B to minimize the Hinge loss, i.e., $\max(1 - yf^{(t)}(\mathbf{X}), 0)$.

Expert specialization. To quantify expert specialization, we define, for each expert s and task-relevant token $\mathbf{v} \in \mathcal{P}_r$, the probability

$$p_{\mathbf{v}}^{(s)} := \mathbb{P} \left[G_j^{(s,t)} \geq 1/l \mid x^{(j)} = \mathbf{v} \text{ for some } j \in [n] \right] \quad (11)$$

over the data distribution \mathcal{D} . A value of $p_{\mathbf{v}}^{(s,t)} = 1$ indicates that the task-relevant token \mathbf{v} is routed to expert s in every sequence containing \mathbf{v} , i.e., expert s is fully specialized on \mathbf{v} .

4.3. Theoretical Generalization Guarantees

Lemma 4.1. *Suppose, the model in (8) is trained for $T = \Theta(l^2 \sqrt{\log l} / \alpha)$ steps. For any $\mathbf{v} \in \{\mathbf{o}_1, \mathbf{o}_2\}$ and any expert s, s' , such that $p_{\mathbf{v}}^{(s,T)} = 1$ and $p_{-\mathbf{v}}^{(s',T)} = 1$, we have*

$$\text{MaxNNScore}^{(s)} < \text{MaxNNScore}^{(s')}$$

Lemma 4.1 shows that, the expert specialized on more-frequent task-relevant token (e.g., the expert s' with $p_{-\mathbf{o}_1}^{(s')} = 1$) maintains larger *maximum neuron norm score* compared to the expert specialized on less-frequent task-relevant token (e.g., the expert s with $p_{\mathbf{o}_1}^{(s)} = 1$).

The weight-programming noise model in (3) indicates that larger weight magnitudes incur higher analog noise, while also corresponding to larger neuron norms. Based on this intuition, we establish formal generalization guarantees for both fully analog and heterogeneous computation in Theorem 4.2.

Theorem 4.2. *Suppose the model given in (8) is trained for $T = \Theta(l^2 \sqrt{\log l} / \alpha)$ steps. Let γ denote the fraction of the experts $s \in [k]$ in the trained model that satisfies $p_{-\mathbf{v}}^{(s,T)} = 1$*

Table 1. Accuracy (%) of MoE models with DAC-ADC noise added to the inputs and outputs of different modules.

Model	Noise	Modules	Tasks								Avg.
			PIQA	ARC-e	ARC-c	BoolQ	HellaS.	Wino.	MathQA	MMLU	
DeepSeek-MoE	Digital (FP-16)	—	80.36	72.85	47.61	72.78	77.38	70.17	31.42	37.67	61.28
	DAC-ADC	Experts	79.16	73.40	47.44	72.57	76.78	69.77	31.22	37.92	61.03
		Experts+Dense	75.68	68.06	39.16	68.29	68.58	60.69	28.17	31.71	55.04
OLMoE	Digital (FP-16)	—	79.71	76.94	49.66	69.85	78.19	68.90	28.44	53.65	63.17
	DAC-ADC	Experts	79.49	76.43	49.49	69.02	77.34	67.72	28.98	51.22	62.46
		Experts+Dense	77.86	74.03	48.89	68.87	77.57	67.88	27.81	50.43	61.54

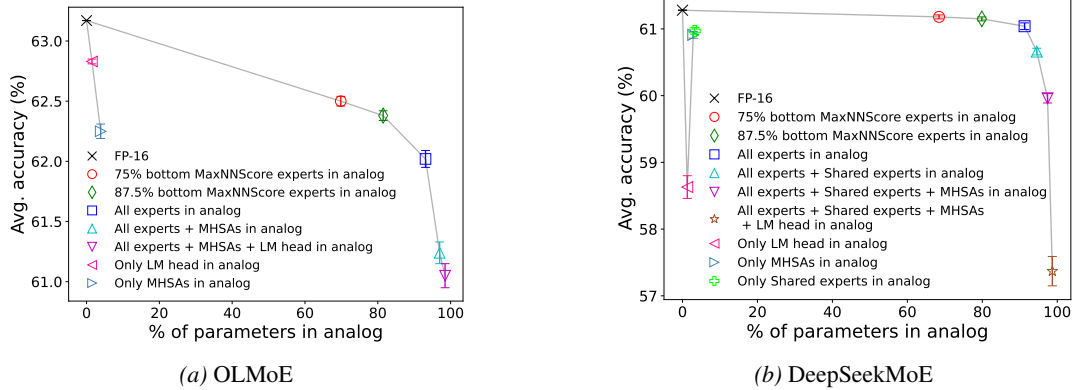


Figure 3. Effect of computing dense modules in analog. Accuracy degradation is significant when densely activated modules are executed on AIMC, despite their small parameter footprint.

for $v \in \{\mathbf{o}_1, \mathbf{o}_2\}$. If the programming-weight magnitude c in the noise model (10) satisfies

$$c \leq c_A := O\left(\frac{\alpha}{1-\alpha} \times \frac{1}{l^2 \sqrt{d \log(kml d^2)}}\right), \quad (12)$$

then with high probability, the Analog-Expert MoE model, denoted by f_A , has guaranteed generalization i.e.,

$$\mathbb{P}[\forall (\mathbf{X}, y) \sim \mathcal{D} : y f_A^{(T)}(\mathbf{X}) > 0] = 1. \quad (13)$$

Moreover, if $\Gamma \geq \gamma$ fraction of the experts with top MaxNNScore are computed in digital while others in analog, and the noise magnitude c satisfies

$$c \leq c_H := \frac{1-\alpha}{\alpha} c_A, \quad (14)$$

then with high probability, the heterogeneous-expert MoE model, denoted by f_H , has guaranteed generalization. i.e.,

$$\mathbb{P}[\forall (\mathbf{X}, y) \sim \mathcal{D} : y f_H^{(T)}(\mathbf{X}) > 0] = 1. \quad (15)$$

Theorem 4.2 characterizes the maximum tolerable programming noise magnitude for guaranteed generalization under

the fully analog and the proposed heterogeneous compute schemes, given in (12) and (14), respectively. It shows that computing a fraction γ of experts in digital, i.e., those specialized on more frequent task-relevant tokens, allows the remaining analog experts to tolerate a programming noise magnitude larger by a factor of $\Omega\left(\frac{1-\alpha}{\alpha}\right)$.

5. Experiments

5.1. Experimental Setup

Evaluated models. We evaluate the robustness of the proposed heterogeneous computation on two large pre-trained MoE LLMs: DeepSeekMoE (Dai et al., 2024) and OLMoE (Muennighoff et al., 2025), with 16B and 7B parameters, respectively. DeepSeekMoE consists of 28 Transformer layers, where the FFN of the first layer is dense and all subsequent FFN blocks are MoE; each MoE block includes a dense shared expert that processes all tokens. OLMoE contains 16 Transformer layers, all with MoE-based FFNs. In both models, each MoE block has 64 sparse experts.

Evaluated task. We test the performance of these models on 8 benchmark LLM tasks: PIQA (Bisk et al., 2020), ARC-Challenge and ARC-Easy (Clark et al., 2018), BoolQ (Clark

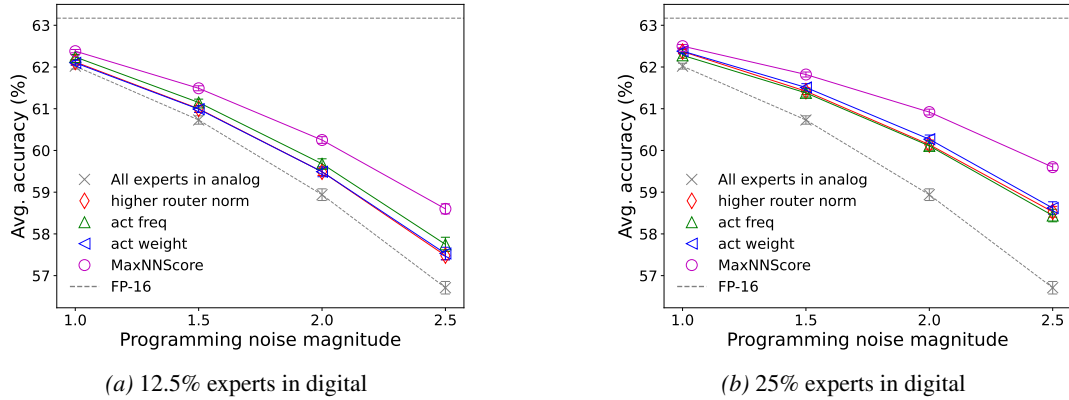


Figure 4. Performance of different digital expert selection methods in OLMoE

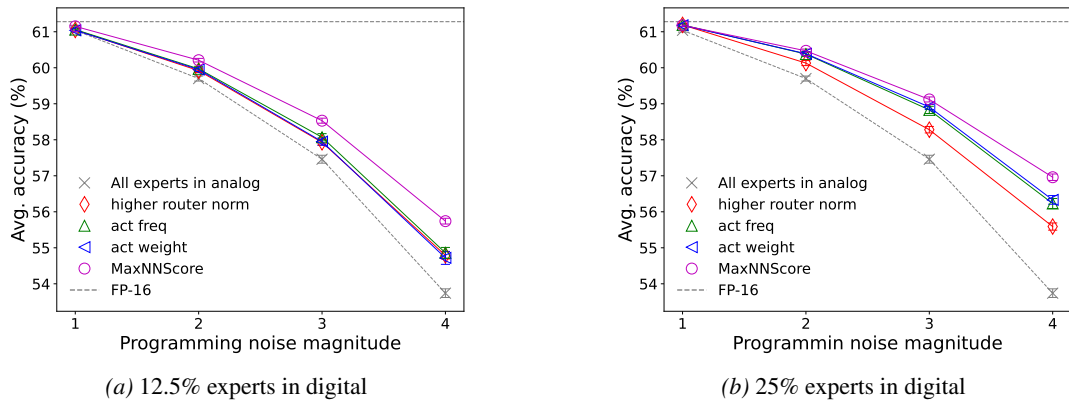


Figure 5. Performance of different digital expert selection methods in DeepSeekMoE

et al., 2019), HellaSwag (Zellers et al., 2019), WinoGrande (Sakaguchi et al., 2021), MathQA (Amini et al., 2019), and MMLU (Hendrycks et al., 2021). These tasks cover diverse areas of LLM capabilities, spanning problem solving in various professional domains, along with commonsense and mathematical reasoning, trivia, and natural language inference.

Analog noise simulation. We simulate the DAC-ADC noise through IBM’s AIHWKIT-Lightning (Büchel et al., 2024). The weight-programming noise is simulated by directly adding Gaussian noise according to (3). For both of the cases, we select the NVM tile size of 512. For programming noise, we report the average and standard error of the results of 32 different random seeds.

5.2. Results on DAC-ADC Noise

We evaluate the robustness of MoE models against DAC-ADC noise. We select 8-bit DAC and ADC for the experiments. Table 1 provides the results of inference accuracy of the two MoE models across eight benchmark LLM tasks, where the DAC-ADC noise is added to the inputs and outputs of different modules. While the models show robust-

ness for noise added to all the experts, adding noise to dense modules significantly degrade performance. The insignificant drop of accuracy (only 0.25% in DeepSeekMoE, and 0.70% drop in OLMoE) for the expert-only case implies that the DAC-ADC noise of the experts can be mitigated to a very low level by properly calibrating the hyperparameters of DAC and ADC. This justifies the design of our digital expert selection strategy based on weight-programming noise.

Given that calibrated DAC-ADC noise is negligible and its simulation is prohibitively slow, we report only weight-programming noise results in the remainder of this section.

5.3. Results on Weight-programming Noise

Effect of computing dense modules in analog. We investigate the relative sensitivity of the dense modules and the sparse expert modules for DeepSeekMoE and OLMoE. The dense modules in OLMoE includes the MHSA modules and the LM head. The DeepSeekMoE includes the additional dense modules of shared expert.

Figure 3 presents the average accuracy of OLMoE and DeepSeekMoE across the eight benchmark LLM tasks, while the standard weight-programming noise given in (3)

Table 2. The throughput, energy efficiency, and accuracy of OLMoE evaluated for batch size 32.

Param. in Digital	Modules in Digital	Throughput (Tokens/s)	Energy Efficiency (Tokens/Watt · s)	Avg. Accuracy (%) vs. Prog. noise magnitude		
				1.0	1.5	2.5
100% (FP-16)	—	4220.07	10.55	63.17		
0% (analog)	None	768.41	23949.07	61.05 ± 0.10	58.45 ± 0.15	49.74 ± 0.23
5.37% (het.gen)	Dense	49781.23	123.92	62.02 ± 0.07	60.73 ± 0.10	56.71 ± 0.15
17.01% (het.gen)	Dense + 12.5% experts	24924.12	62.20	62.38 ± 0.04	61.49 ± 0.06	58.60 ± 0.12
28.65% (het.gen)	Dense + 25.0% experts	14513.52	36.25	62.50 ± 0.04	61.82 ± 0.06	59.60 ± 0.08

is added to different dense modules separately and together with the sparse expert modules. As shown in the figure, despite having a very small percentage of parameters, all of the dense modules shows high sensitivity to the programming noise. In OLMoE, the multi-head self-attention (MHSA) modules account for only 3.88% of the total parameters, yet placing only these modules in analog results in a larger performance degradation than placing 87.5% lower MaxNNScore experts in analog, which comprise 81.5% of the model parameters. Similarly, in DeepSeekMoE, the LM head, the MHSAs, and the shared experts account for 1.28%, 2.87%, and 3.26% of the total parameters, respectively. Yet, placing each of these modules individually in analog results in higher drop than placing 100% of the sparse experts, comprising 91.28% of the total parameters, in analog.

Verifying the effectiveness of the digital expert selection strategy. We compare the performance of our proposed MaxNNScore based digital expert selection strategy against several baselines used for selecting expert for pruning (Koishekenov et al., 2023; Chowdhury et al., 2024) and higher quantized precision (Li et al., 2024b; Huang et al., 2025). We briefly describe the baselines as given below.

Activation Frequency. This metric rank the experts based on their activation frequency, i.e., the fraction of tokens received by each expert over calibration dataset.

Activation Weight. This metric rank the experts based on their average routing weight over calibration dataset.

Router norm. This metric does not require any calibration data. The metric rank the experts based on the norm of their corresponding routing parameters.

Figures 4 and 5 show the average accuracy over the eight benchmark LLM tasks as a function of programming noise magnitude for different expert selection methods, evaluated on OLMoE and DeepSeekMoE, respectively. As shown in the figures, the proposed MaxNNScore based consistently outperforms other baselines, maintaining an increasing gap of accuracy with the noise magnitude. It can be inferred

from the figures that at least one-third of the performance drop can be recovered by placing only one-eighth of the experts in digital, and half of the performance drop can be recovered by placing only one-fourth of the experts in digital.

5.4. Energy Efficiency vs. Throughput vs. Accuracy Tradeoff in Heterogeneous Computation

We evaluate the throughput (Tokens/s), and the energy efficiency (Tokens/Watt-s) for the proposed heterogeneous computing method, and compare with the full analog and full digital compute paradigm. The details about the evaluation of these values are provided in Appendix A.

Heterogeneous computing provides better tradeoff. Table 2 presents the throughput, energy efficiency, and the average accuracy over the eight benchmark tasks under different weight-programming magnitudes for OLMoE. From the table, we can infer that, the full-digital (FP-16) computing is severely energy inefficient, while providing a moderate throughput value. On the other hand, while the full-analog approach’s energy efficiency is incomparably high, it’s generating throughput is the lowest. Note that, unlike digital accelerators, the throughput of full-analog does not increases with batch size, which indicates higher latency for larger batch size. As expected, the approach also suffers from the worst accuracy degradation. However, as observed in the table, the proposed heterogeneous approach provides a balance between throughput and energy efficiency. Moreover, for higher noise magnitudes, computing more experts in digital will allow to trading off some compute efficiency (i.e., throughput and energy efficiency) to achieve higher model performance.

6. Conclusion

In this paper, a heterogeneous computing approach of MoE is provide where the noise sensitive components are computed in digital accelerator, while rest of the components

are computed in analog in-memory devices. We demonstrate that computing dense modules in digital along with the experts of high neuron norm improves model’s robustness against AIMC noises. Furthermore, we show that by varying the experts’ fraction in digital allows flexibility in balancing throughput, energy consumption and accuracy. Future works includes system design for dynamic computation of experts in AIMC and digital accelerators based on the compute and energy budget.

Impact Statement

This work aims to improve the efficiency and robustness of deploying large Mixture-of-Experts models through heterogeneous analog–digital computing. By reducing memory movement and energy consumption while maintaining accuracy, the proposed approach may lower the computational and environmental costs of large-scale model deployment and enable use in more resource-constrained settings. The work does not directly address or exacerbate societal concerns such as bias, fairness, or misuse.

References

- Amini, A., Gabriel, S., Lin, S., Koncel-Kedziorski, R., Choi, Y., and Hajishirzi, H. MathQA: Towards interpretable math word problem solving with operation-based formalisms. In *Proceedings of the 2019 Conference of the North American Chapter of the Association for Computational Linguistics: Human Language Technologies, Volume 1 (Long and Short Papers)*, pp. 2357–2367, Minneapolis, Minnesota, June 2019. Association for Computational Linguistics. doi: 10.18653/v1/N19-1245. URL <https://aclanthology.org/N19-1245>.
- Bisk, Y., Zellers, R., Bras, R. L., Gao, J., and Choi, Y. Piqa: Reasoning about physical commonsense in natural language. In *Thirty-Fourth AAAI Conference on Artificial Intelligence*, 2020.
- Brutzkus, A., Globerson, A., Malach, E., and Shalev-Shwartz, S. Sgd learns over-parameterized networks that provably generalize on linearly separable data. In *International Conference on Learning Representations*, 2018.
- Bu, D., Huang, W., Suzuki, T., Cheng, J., Zhang, Q., Xu, Z., and Wong, H.-S. Provably neural active learning succeeds via prioritizing perplexing samples. In *Proceedings of the 41st International Conference on Machine Learning*, pp. 4642–4695, 2024.
- Büchel, J., Chalas, I., Acampa, G., Chen, A., Fagbohun, O., Tsai, H., Maghraoui, K. E., Gallo, M. L., Rahimi, A., and Sebastian, A. Analog foundation models. In *The Thirty-ninth Annual Conference on Neural Information Processing Systems*, 2025a. URL <https://openreview.net/forum?id=zo4zYTR8vn>.
- Büchel, J., Vasilopoulos, A., Simon, W. A., Boybat, I., Tsai, H., Burr, G. W., Castro, H., Filipiak, B., Le Gallo, M., Rahimi, A., et al. Efficient scaling of large language models with mixture of experts and 3d analog in-memory computing. *Nature Computational Science*, 5(1):13–26, 2025b.
- Burr, G. W., Shelby, R. M., Sebastian, A., Kim, S., Kim, S., Sidler, S., Virwani, K., Ishii, M., Narayanan, P., Fumarola, A., et al. Neuromorphic computing using non-volatile memory. *Advances in Physics: X*, 2(1):89–124, 2017.
- Büchel, J., Simon, W. A., Lammie, C., Acampa, G., Maghraoui, K. E., Gallo, M. L., and Sebastian, A. Aihwkit-lightning: A scalable hw-aware training toolkit for analog in-memory computing. In *NeurIPS 2024 Workshop Machine Learning with new Compute Paradigms*, 2024. URL <https://openreview.net/forum?id=QNdxOgGmhR>.
- Chowdhury, M. N. R., Zhang, S., Wang, M., Liu, S., and Chen, P.-Y. Patch-level routing in mixture-of-experts is provably sample-efficient for convolutional neural networks. In *International Conference on Machine Learning*, pp. 6074–6114. PMLR, 2023.
- Chowdhury, M. N. R., Wang, M., Maghraoui, K. E., Wang, N., Chen, P.-Y., and Carothers, C. A provably effective method for pruning experts in fine-tuned sparse mixture-of-experts. In *Forty-first International Conference on Machine Learning*, 2024. URL <https://openreview.net/forum?id=1oU4FKpVx5>.
- Chowdhury, M. N. R., Wang, M., Maghraoui, K. E., Tsai, H., Wang, N., Burr, G. W., and Liu, L. Efficient quantization of mixture-of-experts with theoretical generalization guarantees. In *The Fourteenth International Conference on Learning Representations*, 2026. URL <https://openreview.net/forum?id=yiMlVBaoQi>.
- Clark, C., Lee, K., Chang, M.-W., Kwiatkowski, T., Collins, M., and Toutanova, K. Boolq: Exploring the surprising difficulty of natural yes/no questions. In *NAACL*, 2019.
- Clark, P., Cowhey, I., Etzioni, O., Khot, T., Sabharwal, A., Schoenick, C., and Tafjord, O. Think you have solved question answering? try arc, the ai2 reasoning challenge. *arXiv:1803.05457v1*, 2018.
- Dai, D., Deng, C., Zhao, C., Xu, R., Gao, H., Chen, D., Li, J., Zeng, W., Yu, X., Wu, Y., et al. Deepseekmoe: Towards ultimate expert specialization in mixture-of-experts language models. In *Proceedings of the 62nd Annual Meeting of the Association for Computational Linguistics (Volume 1: Long Papers)*, pp. 1280–1297, 2024.

- Fedus, W., Zoph, B., and Shazeer, N. Switch transformers: Scaling to trillion parameter models with simple and efficient sparsity. *Journal of Machine Learning Research*, 23(120):1–39, 2022.
- Fernandez, J., Na, C., Tiwari, V., Bisk, Y., Luccioni, S., and Strubell, E. Energy considerations of large language model inference and efficiency optimizations. In *LTI Student Research Symposium 2025*, 2025. URL <https://openreview.net/forum?id=aXNtylYGe0>.
- Frantar, E. and Alistarh, D. Qmoe: Sub-1-bit compression of trillion parameter models. In Gibbons, P., Pekhimenko, G., and Sa, C. D. (eds.), *Proceedings of Machine Learning and Systems*, volume 6, pp. 439–451, 2024.
- Fujiwara, H., Mori, H., Zhao, W.-C., Khare, K., Lee, C.-E., Peng, X., Joshi, V., Chuang, C.-K., Hsu, S.-H., Hashizume, T., et al. 34.4 a 3nm, 32.5 tops/w, 55.0 tops/mm² and 3.78 mb/mm² fully-digital compute-in-memory macro supporting int12× int12 with a parallel-mac architecture and foundry 6t-sram bit cell. In *2024 IEEE International Solid-State Circuits Conference (ISSCC)*, volume 67, pp. 572–574. IEEE, 2024.
- Gokmen, T., Rasch, M. J., and Haensch, W. The marriage of training and inference for scaled deep learning analog hardware. In *2019 IEEE International Electron Devices Meeting (IEDM)*, pp. 22–3. IEEE, 2019.
- Guo, D., Yang, D., Zhang, H., Song, J., Zhang, R., Xu, R., Zhu, Q., Ma, S., Wang, P., Bi, X., et al. Deepseek-r1: Incentivizing reasoning capability in llms via reinforcement learning. *arXiv preprint arXiv:2501.12948*, 2025.
- Hendrycks, D., Burns, C., Basart, S., Zou, A., Mazeika, M., Song, D., and Steinhardt, J. Measuring massive multitask language understanding. *Proceedings of the International Conference on Learning Representations (ICLR)*, 2021.
- Hou, Y., Tsai, H., El Maghraoui, K., Gokmen, T., Burr, G. W., and Liu, L. Nora: Noise-optimized rescaling of llms on analog compute-in-memory accelerators. In *2025 Design, Automation & Test in Europe Conference (DATE)*, pp. 1–7. IEEE, 2025.
- Huang, W., Liao, Y., Liu, J., He, R., Tan, H., Zhang, S., Li, H., Liu, S., and Qi, X. Mixture compressor for mixture-of-experts LLMs gains more. In *The Thirteenth International Conference on Learning Representations*, 2025. URL <https://openreview.net/forum?id=hheFYjOsWO>.
- Jegham, N., Abdelatti, M., Koh, C. Y., Elmoubarki, L., and Hendawi, A. How hungry is ai? benchmarking energy, water, and carbon footprint of llm inference. *arXiv preprint arXiv:2505.09598*, 2025.
- Jiang, A. Q., Sablayrolles, A., Roux, A., Mensch, A., Savary, B., Bamford, C., Chaplot, D. S., Casas, D. d. l., Hanna, E. B., Bressand, F., et al. Mixtral of experts. *arXiv preprint arXiv:2401.04088*, 2024.
- Joshi, V., Le Gallo, M., Haefeli, S., Boybat, I., Piveteau, C., Dazzi, M., Rajendran, B., Sebastian, A., and Eleftheriou, E. Accurate deep neural network inference using computational phase-change memory. *Nature communications*, 11(1):2473, 2020.
- Karp, S., Winston, E., Li, Y., and Singh, A. Local signal adaptivity: Provable feature learning in neural networks beyond kernels. In *Advances in Neural Information Processing Systems*, pp. 24883–24897, 2021.
- Koishekenov, Y., Berard, A., and Nikoulina, V. Memory-efficient nllb-200: Language-specific expert pruning of a massively multilingual machine translation model. In *Proceedings of the 61st Annual Meeting of the Association for Computational Linguistics (Volume 1: Long Papers)*, pp. 3567–3585, 2023.
- Le Gallo, M., Khaddam-Aljameh, R., Stanisavljevic, M., Vasilopoulos, A., Kersting, B., Dazzi, M., Karunaratne, G., Brändli, M., Singh, A., Mueller, S. M., et al. A 64-core mixed-signal in-memory compute chip based on phase-change memory for deep neural network inference. *Nature Electronics*, 6(9):680–693, 2023.
- Li, H., Wang, M., Lu, S., Cui, X., and Chen, P.-Y. How do nonlinear transformers learn and generalize in in-context learning? In *International Conference on Machine Learning*, pp. 28734–28783. PMLR, 2024a.
- Li, H., Lu, S., Chen, P.-Y., Cui, X., and Wang, M. Training nonlinear transformers for chain-of-thought inference: A theoretical generalization analysis. In *The Thirteenth International Conference on Learning Representations*, 2025a. URL <https://openreview.net/forum?id=n7n8McETXw>.
- Li, H., Zhang, Y., Zhang, S., Chen, P.-Y., Liu, S., and Wang, M. When is task vector provably effective for model editing? a generalization analysis of nonlinear transformers. In *The Thirteenth International Conference on Learning Representations*, 2025b.
- Li, P., Jin, X., Cheng, Y., and Chen, T. Examining post-training quantization for mixture-of-experts: A benchmark. *arXiv preprint arXiv:2406.08155*, 2024b.
- Muennighoff, N., Soldaini, L., Groeneveld, D., Lo, K., Morrison, J., Min, S., Shi, W., Walsh, E. P., Tafjord, O., Lambert, N., Gu, Y., Arora, S., Bhagia, A., Schwenk, D., Wadden, D., Wettig, A., Hui, B., Dettmers, T., Kiela, D., Farhadi, A., Smith, N. A., Koh, P. W., Singh, A.,

- and Hajishirzi, H. OLMoe: Open mixture-of-experts language models. In *The Thirteenth International Conference on Learning Representations*, 2025. URL <https://openreview.net/forum?id=xXTkbTBmqg>.
- Rasch, M. J., Mackin, C., Le Gallo, M., Chen, A., Fasoli, A., Odermatt, F., Li, N., Nandakumar, S., Narayanan, P., Tsai, H., et al. Hardware-aware training for large-scale and diverse deep learning inference workloads using in-memory computing-based accelerators. *Nature communications*, 14(1):5282, 2023.
- Riquelme, C., Puigcerver, J., Mustafa, B., Neumann, M., Jenatton, R., Susano Pinto, A., Keysers, D., and Houlsby, N. Scaling vision with sparse mixture of experts. *Advances in Neural Information Processing Systems*, 34: 8583–8595, 2021.
- Sakaguchi, K., Bras, R. L., Bhagavatula, C., and Choi, Y. Winogrande: An adversarial winograd schema challenge at scale. *Communications of the ACM*, 64(9):99–106, 2021.
- Sebastian, A., Le Gallo, M., Khaddam-Aljameh, R., and Eleftheriou, E. Memory devices and applications for in-memory computing. *Nature nanotechnology*, 15(7): 529–544, 2020.
- Shazeer, N., Mirhoseini, A., Maziarz, K., Davis, A., Le, Q., Hinton, G., and Dean, J. Outrageously large neural networks: The sparsely-gated mixture-of-experts layer. In *International Conference on Learning Representations*, 2017.
- Shi, Z., Wei, J., and Liang, Y. A theoretical analysis on feature learning in neural networks: Emergence from inputs and advantage over fixed features. In *International Conference on Learning Representations*, 2022.
- Spoon, K., Tsai, H., Chen, A., Rasch, M. J., Ambrogio, S., Mackin, C., Fasoli, A., Friz, A. M., Narayanan, P., Stanisavljevic, M., et al. Toward software-equivalent accuracy on transformer-based deep neural networks with analog memory devices. *Frontiers in Computational Neuroscience*, 15:675741, 2021.
- Tsai, H., Ambrogio, S., Mackin, C., Narayanan, P., Shelby, R. M., Rocki, K., Chen, A., and Burr, G. W. Inference of long-short term memory networks at software-equivalent accuracy using 2.5 m analog phase change memory devices. In *2019 Symposium on VLSI Technology*, pp. T82–T83. IEEE, 2019.
- Wan, W., Kubendran, R., Schaefer, C., Eryilmaz, S. B., Zhang, W., Wu, D., Deiss, S., Raina, P., Qian, H., Gao, B., et al. A compute-in-memory chip based on resistive random-access memory. *Nature*, 608(7923):504–512, 2022.
- Yang, A., Li, A., Yang, B., Zhang, B., Hui, B., Zheng, B., Yu, B., Gao, C., Huang, C., Lv, C., et al. Qwen3 technical report. *arXiv preprint arXiv:2505.09388*, 2025.
- Zellers, R., Holtzman, A., Bisk, Y., Farhadi, A., and Choi, Y. Hellaswag: Can a machine really finish your sentence? In *Proceedings of the 57th Annual Meeting of the Association for Computational Linguistics*, 2019.
- Zhang, B., Chen, C.-Y., and Verma, N. Reshape and adapt for output quantization (RAOQ): Quantization-aware training for in-memory computing systems. In Salakhutdinov, R., Kolter, Z., Heller, K., Weller, A., Oliver, N., Scarlett, J., and Berkenkamp, F. (eds.), *Proceedings of the 41st International Conference on Machine Learning*, volume 235 of *Proceedings of Machine Learning Research*, pp. 58739–58762. PMLR, 21–27 Jul 2024. URL <https://proceedings.mlr.press/v235/zhang24i.html>.
- Zhou, Y., Lei, T., Liu, H., Du, N., Huang, Y., Zhao, V. Y., Dai, A. M., Chen, Z., Le, Q. V., and Laudon, J. Mixture-of-experts with expert choice routing. In Oh, A. H., Agarwal, A., Belgrave, D., and Cho, K. (eds.), *Advances in Neural Information Processing Systems*, 2022.

A. The Details for Evaluating Throughput and Energy Efficiency

To evaluate the two quantities, we consider that the digital accelerator is equivalent to an NVIDIA A100 GPU. The quantities are evaluated under 100% model FLOPs utilization (MFU), with 624 tera operations per second (624 TOP/s) at 400Watt, and with data transfer bandwidth of 1,555 GB/s for the accelerator. In that case, the throughput is evaluated as,

$$\text{Throughput (tokens/s)} = \frac{\text{No. of tokens generated}}{\max\left(\frac{\text{Total TOPs}}{\text{MFU}624\text{TOPs/s}}, \frac{\text{Total weight transfer}}{1555\text{GB/s}}\right)} \tag{16}$$

The energy efficiency can be directly calculated using the throughput and power rating of the device.

For the analog accelerator, we compute the throughput by dividing the total number of tokens generated during inference by the total latency accumulated over all the asynchronous operations in forward passes. Similarly, the energy efficiency is evaluated by dividing the number of tokens generated by the total energy consumption accumulated over all operations in forward passes. The latencies and energy consumption values for different operations are taken from (Büchel et al., 2025b).

For the heterogeneous case, we take the upper-bound of the latencies over both accelerators, and the energy consumption is evaluated by adding the product of the digital accelerator’s power rating and latency to analog accelerator’s energy consumption.

B. Hyperparameter Calibration Results for DAC and ADC

We calibrate the hyperparameter κ and λ to obtain the results in Table 1, according to the method described in section 2.2. We use Wkitext-103 test set for calibration. The results are given in

Table 3. κ vs. Perplexity (PPL) for OLMoE. Noise added only at the experts.

κ	10	18	25	30	35	40	45	50
PPL	10.98	7.59	7.10	7.00	6.97	6.99	7.02	7.07

Table 4. λ vs. Perplexity (PPL) for OLMoE ($\kappa = 35$). Noise added only at the experts.

λ	0.75	0.9	1.0	1.125	1.25	1.5	1.75	2.0	2.25	2.5	2.75
PPL	7.15	7.10	7.10	7.11	7.13	7.19	7.26	7.32	7.42	7.48	7.57

Table 5. κ vs. Perplexity (PPL) for OLMoE. Noise added to both experts and dense modules.

κ	10	15	20	25	30	35	40	45
PPL	22.26	8.66	7.50	7.16	7.07	7.07	7.12	7.18

Table 6. λ vs. Perplexity (PPL) for OLMoE ($\kappa = 30$). Noise added to experts and dense modules.

λ	0.75	1.0	1.25	1.5
PPL	7.42	7.26	7.28	7.38

Table 7. κ vs. Perplexity (PPL) for DeepSeekMoE. Noise added to experts.

κ	30	35	40	45	50	60
PPL	6.64	6.62	6.62	6.63	6.64	6.68

Table 8. λ vs. Perplexity (PPL) for DeepSeekMoE ($\kappa = 40$). Noise added to experts only.

λ	0.9	1.0	1.25	1.5	2.0	2.25	2.5	3.0	4.0
PPL	6.97	6.86	6.73	6.69	6.68	6.67	6.67	6.69	6.76

Table 9. κ vs. Perplexity (PPL) for DeepSeekMoE. Noise added to experts and dense modules.

κ	30	35	40	45	50
PPL	7.06	7.05	7.09	7.18	7.30

Table 10. λ vs. Perplexity (PPL) for DeepSeekMoE ($\kappa = 35$). Noise added to experts and dense modules.

λ	1.0	1.25	1.5	1.75	2.0	2.25
PPL	7.75	7.52	7.51	7.58	7.70	7.85

C. Token Visualization of Neurons Corresponding to MaxNNorm



Figure 6. Token visualization of the first MoE block of OLMoE. Expert 30, 50, and 14 correspond to lowest three $MaxNNorm$ neurons over the up-projection matrices. Similarly, Expert 38, 57, and 6 correspond to the highest $MaxNNorm$ neurons over the up-projection matrices.

We visualize the top activating tokens of the neurons corresponding to maximum neuron norm for OLMoE. Figure 6 presents the results for the first layer of the model. Expert 30, 50, and 14 are the lowest $MaxNNorm$ experts for the up-projection matrices. Expert 38, 57, and 6 are highest $MaxNNorm$ experts for the up-projection layers. As we can see, the lowest neuron norm experts are activating by semantically less-frequent tokens (e.g., 'ach', 'ell', 'Ireland', 'ite', 'erry' etc.). On the other hand highest neuron norm experts are activating to semantically more-frequent tokens (e.g., 'the', 'a', 'this', 'them', 'each', 'and', etc.). This justify our intuition that higher $MaxNNorm$ experts specialize to more-frequent tokens.

D. Preliminaries

For theoretical analysis, we adopt exactly the same setting as in (Chowdhury et al., 2026). We re-state the setting here.

As we theoretically analyze the expert-choice routing, for any training step t , equation (8) can be re-written as,

$$f^{(t)}(\mathbf{X}) = \sum_{s=1}^k f_s^{(t)}(\mathbf{X}), \text{ where } f_s^{(t)}(\mathbf{X}) = a^{(s)} \sum_{j \in J_s^{(t)}(\mathbf{X})} G_j^{(s,t)} \sum_{r=1}^m \phi(\langle \mathbf{w}_r^{(s,t)}, \mathbf{x}^{(j)} \rangle) \quad (17)$$

where, $J_s^{(t)}(\mathbf{X})$ is the set of tokens routed to expert s at step t , $\mathbf{w}_r^{(s,t)}$ is the r -th neuron of $\mathbf{W}_{\text{up}}^{(s)}$ at step t , and $\mathbf{x}^{(j)}$ is the j -th token of the sequence \mathbf{X} .

Tokens with top l routing scores, i.e., the tokens of \mathbf{X} with top l indices of $[\mathbf{X}^\top \boldsymbol{\Sigma}]_{:,s}$ are routed to expert s .

We consider $\phi = \text{ReLU}(\cdot)$, i.e., the rectified linear unit. The routing weight of j -th token at expert s can be calculated as,

$$G_j^{(s,t)} = \begin{cases} \frac{\exp(\langle \mathbf{w}_s^{(t)}, \mathbf{x}^{(j)} \rangle)}{\sum_{i \in J_s^{(t)}(\mathbf{X})} \exp(\langle \mathbf{w}_s^{(t)}, \mathbf{x}^{(i)} \rangle)}, & j \in J_s^{(t)}(\mathbf{X}), \\ 0, & \text{otherwise.} \end{cases} \quad (18)$$

Here, $\mathbf{w}_s^{(t)} = \boldsymbol{\Sigma}_{:,s}^{(t)}$ is the routing vector corresponding to the expert s at step t .

The model is trained to minimize the Hinge loss

$$\hat{l}^{(t)}(\mathbf{X}, y) = \max(1 - yf^{(t)}(\mathbf{X}), 0) \quad (19)$$

while the gradients are evaluated on

$$l^{(t)}(\mathbf{X}, y) = 1 - yf^{(t)}(\mathbf{X}) \quad (20)$$

For any input (\mathbf{X}, y) , the gradient for $\mathbf{w}_r^{(s,t)}$ is evaluated as,

$$\frac{\partial l^{(t)}(\mathbf{X}, y)}{\partial \mathbf{w}_r^{(s,t)}} = -ya^{(s)} \sum_{j \in J_s^{(t)}(\mathbf{X})} G_j^{(s,t)} \mathbf{x}^{(j)} \mathbf{1}_{\langle \mathbf{w}_r^{(s,t)}, \mathbf{x}^{(j)} \rangle \geq 0} \quad (21)$$

The model is trained via Stochastic Gradient Descent algorithm (SGD) with batch size B . The expert weights are updated with learning rate η_e , and the routing parameters are updated with a learning rate η_r . The batch gradient for $\mathbf{w}_r^{(s,t)}$ is evaluated as,

$$\frac{\partial l}{\partial \mathbf{w}_r^{(s,t)}} = \frac{1}{B} \sum_{\mathbf{X} \in \mathcal{B}_t} \frac{\partial l^{(t)}(\mathbf{X}, y)}{\partial \mathbf{w}_r^{(s,t)}} \quad (22)$$

Notations:

1. $\tilde{O}(\cdot)$ and $\tilde{\Omega}(\cdot)$ hides the factor $\log(\text{poly}(d))$ with a sufficiently large polynomial $\text{poly}(\cdot)$
2. With high probability (abbreviated as *w.h.p.*) refers to the probability $1 - \frac{1}{\text{poly}(d)}$.

Definitions:

For any $\mathbf{v} \in \mathcal{P}_r$, we define a complementary expert proficiency measure for the expert s at time t as,

$$\bar{p}_{\mathbf{v}}^{(s,t)} := \mathbb{P} \left[(\mathbf{X}, y) \sim \mathcal{D} : \exists j \in J_s^{(t)} \text{ such that } \mathbf{x}^{(j)} = \mathbf{v} \mid \exists j \in [n] \text{ such that } \mathbf{x}^{(j)} = \mathbf{v} \right].$$

Without the loss of generality, we assume that for any $s \in S_{\mathbf{v}}$, $\bar{p}_{-\mathbf{v}}^{(s,0)} = O(1/d)$.

We define $C_n := \max \left\{ \left\| \mathbf{w}_r^{(s,0)} \right\| \right\}_{s \in [k], r \in [m]}$.

We define, $\gamma_{\mathbf{v}} := \frac{|S_{\mathbf{v}}|}{|S_+|}$ for $\mathbf{v} \in \{\pm \mathbf{o}_1\}$ and $\gamma_{\mathbf{v}} := \frac{|S_{\mathbf{v}}|}{|S_-|}$ for $\mathbf{v} \in \{\pm \mathbf{o}_2\}$.

Therefore, $\gamma = \max\{\gamma_{\mathbf{v}}\}_{\mathbf{v} \in \{\mathbf{o}_1, \mathbf{o}_2\}}$.

Without the loss of generality, we assume that $\forall \mathbf{v} \in \mathcal{P}_r, \gamma_{\mathbf{v}} = \Omega(1)$.

We define, $C_p := \min\{\langle \mathbf{w}_s^{(0)}, \mathbf{q} - \mathbf{q}' \rangle\}_{s \in [k], \mathbf{q} \in \mathcal{P} \cup \{-\mathbf{o}_1, -\mathbf{o}_2\}, \mathbf{q}' \in \mathcal{P} \cup \{-\mathbf{o}_1, -\mathbf{o}_2\} \setminus \{\mathbf{q}\}}$.

We assume that $C_p > 0$.

We assume that for any $\mathbf{v} \in \mathcal{P}_r$ and any $s \in S_{\mathbf{v}}$, $\frac{|\{r \in [m] : \langle \mathbf{w}_r^{(s,0)}, \mathbf{v} \rangle \geq 0\}|}{m} = \Omega(1)$, and $||S_+| - |S_-|| = O(\sqrt{k})$.

We define,

- $G_{\mathbf{v}}^{(s,t)}$: Routing weights of the token $x^{(j)} = \mathbf{v}$ for some $j \in [n]$ and $\mathbf{v} \in \mathcal{P}_r$ at expert s and step t
- $G_{\mathbf{q}}^{(s,t)}$: Routing weights of the token $x^{(j)} = \mathbf{q}$ for some $j \in [n]$ and $\mathbf{q} \in \mathcal{P} \setminus \{\mathbf{o}_1, \mathbf{o}_2\}$ at expert s and step t
- $l_{\mathbf{q}}^{(s,t)} := \left| \{j \in J_s^{(t)}(\mathbf{X}) : \mathbf{x}^{(j)} = \mathbf{q}\} \right|$, is the number of copies of the task-irrelevant vector $\mathbf{q} \in \mathcal{P} \setminus \{\mathbf{o}_1, \mathbf{o}_2\}$ in the set of top l tokens for the input sequence \mathbf{X} at expert s and step t

Components of the neurons' gradients.

For any input $(\mathbf{X}, y) \sim \mathcal{D}$, the gradient component of $\mathbf{w}_r^{(s,t)}$ along any task-relevant vector $\mathbf{v} \in \mathcal{P}_r$ and along any task-irrelevant vector $\mathbf{q} \in \mathcal{P} \setminus \{\mathbf{o}_1, \mathbf{o}_2\}$ at iteration t are evaluated as follows:

$$\left\langle \frac{\partial l(\mathbf{X}, y)}{\partial \mathbf{w}_r^{(s,t)}}, \mathbf{q} \right\rangle = \begin{cases} 0 & \text{if } \langle \mathbf{w}_r^{(s,t)}, \mathbf{q} \rangle < 0 \\ 0 & \text{if } \langle \mathbf{w}_r^{(s,t)}, \mathbf{q} \rangle \geq 0 \text{ but, } \nexists j \in J_s^{(t)}(\mathbf{X}) \text{ s.t. } \mathbf{x}^{(j)} = \mathbf{q} \\ -y a^{(s)} l_{\mathbf{q}}^{(s,t)} G_{\mathbf{q}}^{(s,t)} & \text{if } \langle \mathbf{w}_r^{(s,t)}, \mathbf{q} \rangle \geq 0 \text{ and, } \exists j \in J_s^{(t)}(\mathbf{X}) \text{ s.t. } \mathbf{x}^{(j)} = \mathbf{q} \end{cases} \quad (23)$$

$$\left\langle \frac{\partial l(\mathbf{X}, y)}{\partial \mathbf{w}_r^{(s,t)}}, \mathbf{v} \right\rangle = \begin{cases} 0 & \text{if } \langle \mathbf{w}_r^{(s,t)}, \mathbf{v} \rangle < 0 \text{ but } \nexists j \in J_s^{(t)}(\mathbf{X}) \text{ s.t. } \mathbf{x}^{(j)} = -\mathbf{v} \\ y a^{(s)} G_{-\mathbf{v}}^{(s,t)}(\mathbf{X}) & \text{if } \langle \mathbf{w}_r^{(s,t)}, \mathbf{v} \rangle < 0 \text{ and } \exists j \in J_s^{(t)}(\mathbf{X}) \text{ s.t. } \mathbf{x}^{(j)} = -\mathbf{v} \\ 0 & \text{if } \langle \mathbf{w}_r^{(s,t)}, \mathbf{v} \rangle \geq 0 \text{ but } \nexists j \in J_s^{(t)}(\mathbf{X}) \text{ s.t. } \mathbf{x}^{(j)} = \mathbf{v} \\ -y a^{(s)} G_{\mathbf{v}}^{(s,t)}(\mathbf{X}) & \text{if } \langle \mathbf{w}_r^{(s,t)}, \mathbf{v} \rangle \geq 0 \text{ and } \exists j \in J_s^{(t)}(\mathbf{X}) \text{ s.t. } \mathbf{x}^{(j)} = \mathbf{v} \end{cases} \quad (24)$$

Lemma D.1 (Lemma J.5(ii) of (Chowdhury et al., 2026)). *For any expert $s \in S_{\mathbf{v}}$ such that $\mathbf{v} \in \{\mathbf{o}_1, \mathbf{o}_2\}$, and $\forall \mathbf{q} \in \mathcal{P} \setminus \{\mathbf{o}_1, \mathbf{o}_2\}$, by selecting $\eta_r = O\left(\frac{\eta_e C_p}{ml^2 C_n^2}\right)$ and $B = \tilde{\Omega}(d^2)$, we can ensure that after $T' = O\left(\frac{lC_2}{\alpha \eta_e}\right)$ steps, $p_{\mathbf{v}}^{(s, T')} \geq p_{\mathbf{v}}^{(s, 0)}$ and, $\bar{p}_{-\mathbf{v}}^{(s, T')} \leq \bar{p}_{-\mathbf{v}}^{(s, 0)}$.*

Lemma D.2 (Lemma J.6(ii) of (Chowdhury et al., 2026)). *For any expert $s \in S_{\mathbf{v}}$ such that $\mathbf{v} \in \{-\mathbf{o}_1, -\mathbf{o}_2\}$, and $\forall \mathbf{q} \in \mathcal{P} \setminus \{\mathbf{o}_1, \mathbf{o}_2\}$, by selecting $\eta_r = O\left(\frac{\eta_e C_p}{ml^2 C_n^2}\right)$ and $B = \tilde{\Omega}(d^2)$, we can ensure that after $T' = O\left(\frac{lC_n}{(1-\alpha)\eta_e}\right)$ steps, $p_{\mathbf{v}}^{(s, T')} \geq p_{\mathbf{v}}^{(s, 0)}$ and, $\bar{p}_{-\mathbf{v}}^{(s, T')} \leq \bar{p}_{-\mathbf{v}}^{(s, 0)}$.*

Lemma D.3 (Lemma I.1(i) of (Chowdhury et al., 2026)). *After $T = \Theta(l^2 C_n \sqrt{\log l} / \alpha \eta_e \sqrt{C_p})$ steps of SGD with batch size $B = \tilde{\Omega}(d^2)$ and $\eta_r = O\left(\frac{\eta_e C_p}{ml^2 C_n^2}\right)$, for all $s \in S_v$ and $\mathbf{v} \in \mathcal{P}_r = \{\pm \mathbf{o}_1, \pm \mathbf{o}_2\}$, we have $p_{\mathbf{v}}^{(s,T)} = 1$, $\bar{p}_{-\mathbf{v}}^{(s,T)} = 0$, and $\forall \mathbf{x}^{(j)} = \mathbf{v}$ for some $j \in [n]$, $G_j^{(s,T)} > \frac{1}{2}$.*

E. Proof of Lemma 4.1

Lemma E.1 (Full version of Lemma 4.1). *Suppose, the network given in (8) is trained for $T = \Theta(l^2 C_n \sqrt{\log l} / \alpha \eta_e \sqrt{C_p})$ steps with batch size $B = \tilde{\Omega}(d^2)$ and $\eta_r = O\left(\frac{\eta_e C_p}{ml^2 C_n^2}\right)$. Then, for any $\mathbf{v} \in \{\mathbf{o}_1, \mathbf{o}_2\}$ and any expert s, s' , such that $p_{\mathbf{v}}^{(s,T)} = 1$ and $p_{-\mathbf{v}}^{(s',T)} = 1$, we have*

$$\text{MaxNNScore}^{(s)} < \text{MaxNNScore}^{(s')} \quad (25)$$

Proof. From Lemma D.3, for any $s \in S_+$, and for any $\mathbf{v} \in \{\mathbf{o}_1, -\mathbf{o}_1\}$, if $p_{\mathbf{v}}^{(s,T)} = 1$, then $s \in S_v$.

Similarly, for any $s \in S_-$, and for any $\mathbf{v} \in \{\mathbf{o}_2, -\mathbf{o}_2\}$, if $p_{\mathbf{v}}^{(s,T)} = 1$, then $s \in S_v$.

Now, WLOG let us assume $s \in S_{\mathbf{o}_1}$ and $s' \in S_{-\mathbf{o}_1}$.

Then, using Lemma D.1, $\forall r \in [m], \forall t \leq T$, $\left| \left\langle \frac{\partial l}{\partial \mathbf{w}_r^{(s,t)}}, \mathbf{o}_1 \right\rangle \right| \leq \frac{\alpha}{2} + \tilde{O}\left(\frac{1}{\sqrt{B}}\right)$, which implies, for $B = \tilde{\Omega}(d^2)$, $\forall r \in [m]$, $\left| \langle \mathbf{w}_r^{(s,T)}, \mathbf{o}_1 \rangle \right| = O(l^2 C_n \sqrt{\log l} / \eta_e \sqrt{C_p})$.

On the other hand, $\forall r \in [m], \forall t \leq T$, if $\langle \mathbf{w}_r^{(s,t)}, \mathbf{o}_2 \rangle \geq 0$, then $\left\langle \frac{\partial l}{\partial \mathbf{w}_r^{(s,t)}}, \mathbf{o}_2 \right\rangle \geq 0$, and if $\langle \mathbf{w}_r^{(s,t)}, \mathbf{o}_2 \rangle \leq 0$, then $\left\langle \frac{\partial l}{\partial \mathbf{w}_r^{(s,t)}}, -\mathbf{o}_2 \right\rangle \geq 0$. Therefore, $\left| \langle \mathbf{w}_r^{(s,T)}, \mathbf{o}_2 \rangle \right| = O(C_n)$.

Again, for any $\mathbf{q} \in \mathcal{P} \setminus \{\mathbf{o}_1, \mathbf{o}_2\}$, $\forall r \in [m], \forall t \leq T$, $\left| \left\langle \frac{\partial l}{\partial \mathbf{w}_r^{(s,t)}}, \mathbf{q} \right\rangle \right| \leq O\left(\frac{1}{d}\right) + \tilde{O}\left(\frac{1}{\sqrt{B}}\right)$, which implies, $\left| \langle \mathbf{w}_r^{(s,T)}, \mathbf{q} \rangle \right| = O(C_n)$.

Therefore, $\text{MaxNNScore}^{(s)} = O(l^2 C_n \sqrt{\log l} / \sqrt{C_p})$.

Now, as Lemma D.2 holds, $\forall r \in [m]$ such that $\langle \mathbf{w}_r^{(s',t)}, -\mathbf{o}_1 \rangle \geq 0$,

$$\forall t \geq \frac{\alpha T}{1 - \alpha}, \left\langle \frac{\partial l}{\partial \mathbf{w}_r^{(s',0)}}, -\mathbf{o}_1 \right\rangle \leq -\Omega(1 - \alpha) + \tilde{O}\left(\frac{1}{\sqrt{B}}\right).$$

Therefore, $\forall r \in [m]$ such that $\langle \mathbf{w}_r^{(s',0)}, -\mathbf{o}_1 \rangle \geq 0$, $\langle \mathbf{w}_r^{(s',T)}, -\mathbf{o}_1 \rangle = \Omega((1 - 2\alpha)l^2 C_n \sqrt{\log l} / \alpha \sqrt{C_p})$.

Therefore, $\text{MaxNNScore}^{(s')} = \Omega((1 - 2\alpha)l^2 C_n \sqrt{\log l} / \alpha \sqrt{C_p})$ which completes the proof. \square

F. Proof of Theorem 4.2

Theorem F.1 (Full version of Theorem 4.2). *Suppose, the network given in (8) is trained for $T = \Theta(l^2 C_n \sqrt{\log l} / \alpha \eta_e \sqrt{C_p})$ steps with batch size $B = \tilde{\Omega}(d^2)$ and $\eta_r = O\left(\frac{\eta_e C_p}{ml^2 C_n^2}\right)$. Suppose, γ fraction of the experts $s \in [k]$ in the trained model satisfies $p_{-\mathbf{v}}^{(s,T)} = 1$ for $v \in \{\mathbf{o}_1, \mathbf{o}_2\}$. If*

$$c \leq c_A := O\left(\frac{\alpha}{1 - \alpha} \times \frac{1}{l^2 \sqrt{d \log(kml d^2)}}\right) \quad (26)$$

with high probability the analog model has guaranteed generalization i.e., $\mathbb{P}[\forall(\mathbf{X}, y) \sim \mathcal{D} : yf_A^{(T)}(\mathbf{X}) > 0] = 1$. Furthermore, computing $\Gamma \geq \gamma$ fraction of the experts with top MaxNNScore in digital, if

$$c \leq c_H := \frac{1 - \alpha}{\alpha} c_A \quad (27)$$

with high probability the heterogeneous model has guaranteed generalization i.e., $\mathbb{P}[\forall(\mathbf{X}, y) \sim \mathcal{D} : yf_H^{(T)}(\mathbf{X}) > 0] = 1$.

Proof. For any $r \in [m]$ of $s \in [k]$, the analog weights $\hat{\mathbf{w}}_r^{(s,T)} = \mathbf{w}_r^{(s,T)} + \Delta \mathbf{w}$ where, $\Delta \mathbf{w}$ is the programming error.

Now, for any $\mathbf{q} \in \mathcal{P}$, $\langle \Delta \mathbf{w}, \mathbf{q} \rangle \sim \mathcal{N}(0, \sigma^2)$, where $\sigma \leq \sqrt{d} c_0 \max(\mathbf{w}_r^{(s,T)})$.

Now, from Lemma D.3, for any $s_1 \in S_{\mathbf{o}_1}$, $p_{\mathbf{o}_1}^{(s_1, T)} = 1$ and $\forall \mathbf{x}^{(j)} = \mathbf{o}_1$ for some $j \in [n]$, $G_j^{(s_1, T)} \geq \frac{1}{2}$.

Furthermore, $\sum_{r \in [m]} \langle \mathbf{w}_r^{(s_1, T)}, \mathbf{o}_1 \rangle = \Omega(mlC_2 \sqrt{\frac{\log l}{C_p}})$.

Therefore, for any $(\mathbf{X}, y) \sim \mathcal{D}$ such that $\exists j \in [n]$ with $\mathbf{x}^{(j)} = \mathbf{o}_1$,

$$\sum_{s_1 \in S_{\mathbf{o}_1}} f_{s_1}^{(T)}(\mathbf{X}) = \Omega(\gamma_{\mathbf{o}_1} mlC_n \sqrt{\frac{\log l}{C_p}}).$$

On the other hand, from statement (i) of Lemma D.3, for any $s_3 \in S_{-\mathbf{o}_1}$, $p_{\mathbf{o}_1}^{(s_3, T)} = 0$.

Therefore, for any $(x, y) \sim \mathcal{D}$ such that $\exists j \in [n]$ with $x^{(j)} = \mathbf{o}_1$,

$$\sum_{s \in S_+} f_s^{(T)}(x) = \Omega(\gamma_{\mathbf{o}_1} kmlC_2 \sqrt{\frac{\log l}{C_p}}).$$

Again, for any $q \in \mathcal{P} \setminus \{\mathbf{o}_1, \mathbf{o}_2\}$, $\forall s \in [k]$, $\sum_{r \in [m]} \langle \mathbf{w}_r^{(s, T)}, \mathbf{q} \rangle = O(mC_n)$, and $\forall s \in S_-$, $\sum_{r \in [m]} \langle \mathbf{w}_r^{(s, T)}, \mathbf{o}_1 \rangle = O(mC_n)$.

Therefore, for any $(\mathbf{X}, y) \sim \mathcal{D}$ such that $\exists j \in [n]$ with $\mathbf{x}^{(j)} = \mathbf{o}_1$, $f^{(T)}(\mathbf{X}) = \Omega(\gamma_{\mathbf{o}_1} kmlC_n \sqrt{\frac{\log l}{C_p}}) - O(klmC_n)$, which implies for any $(\mathbf{X}, y) \sim \mathcal{D}$ such that $\exists j \in [n]$ with $\mathbf{x}^{(j)} = \mathbf{o}_1$, $yf^{(T)}(\mathbf{X}) > 0$.

(Condition 1) Therefore, to ensure that for any $(\mathbf{X}, y) \sim \mathcal{D}$ such that $\exists j \in [n]$ with $\mathbf{x}^{(j)} = \mathbf{o}_1$, $yf_A^{(T)}(\mathbf{X}) > 0$, we need

$$f^{(T)}(\mathbf{X}) - f_A^{(T)}(\mathbf{X}) = O(kmlC_n \sqrt{\frac{\log l}{C_p}}).$$

(Condition 2) Similarly, to ensure that for any $(\mathbf{X}, y) \sim \mathcal{D}$ such that $\exists j \in [n]$ with $\mathbf{x}^{(j)} = -\mathbf{o}_1$, $yf_A^{(T)}(\mathbf{X}) > 0$, we need

$$f^{(T)}(\mathbf{X}) - f_A^{(T)}(\mathbf{X}) = O\left(\frac{1 - \alpha}{\alpha} kmlC_n \sqrt{\frac{\log l}{C_p}}\right).$$

Now, for any $s_1 \in S_{\mathbf{o}_1}$, $\text{MaxNNScore}^{(s_1)} = O(l^2 C_n \sqrt{\frac{\log l}{C_p}})$, and $s_3 \in S_{-\mathbf{o}_1}$ $\text{MaxNNScore}^{(s_3)} =$

$$O\left(\frac{1 - \alpha}{\alpha} l^2 C_n \sqrt{\frac{\log l}{C_p}}\right), \text{ which implies for any } r \in [m], \max(\mathbf{w}_r^{(s_1, T)}) \leq O(l^2 C_n \sqrt{\frac{\log l}{C_p}}), \text{ and } \max(\mathbf{w}_r^{(s_3, T)}) \leq$$

$$O\left(\frac{1 - \alpha}{\alpha} l^2 C_n \sqrt{\frac{\log l}{C_p}}\right).$$

Similarly, for any $s_2 \in S_{\mathbf{o}_2}$, $\text{MaxNNScore}^{(s_2)} = O(l^2 C_n \sqrt{\frac{\log l}{C_p}})$, and $s_4 \in S_{-\mathbf{o}_2}$ $\text{MaxNNScore}^{(s_4)} =$

$$O\left(\frac{1-\alpha}{\alpha}l^2C_n\sqrt{\frac{\log l}{C_p}}\right), \text{ which implies for any } r \in [m], \max(\mathbf{w}_r^{(s_2, T)}) \leq O(l^2C_n\sqrt{\frac{\log l}{C_p}}), \text{ and } \max(\mathbf{w}_r^{(s_4, T)}) \leq O\left(\frac{1-\alpha}{\alpha}l^2C_n\sqrt{\frac{\log l}{C_p}}\right).$$

Therefore, to ensure that both condition 1 and condition 2 hold with probability $1 - \frac{1}{d^2}$ over the randomness of programming noise, we need $c_A = O\left(\frac{\alpha}{1-\alpha} \times \frac{1}{l^2\sqrt{d\log(kmld^2)}}\right)$.

Now as Lemma D.3 holds, placing γ fraction of the experts with top MaxNNScore in digital, i.e., we need $c_H = O\left(\frac{1}{l^2\sqrt{d\log(kmld^2)}}\right)$ to ensure condition 1 and 2 hold with probability at least $1 - \frac{1}{d^2}$.

□